

ARTICLE

Color Subtractive–Computer-assisted Image Analysis for Quantification of Cutaneous Nerves in a Diabetic Mouse Model

Robert A. Underwood, Nicole S. Gibran, Lara A. Muffley, Marcia L. Usui, and John E. Olerud

Departments of Medicine (Dermatology) (RAU,LAM,MLU,JEO) and Surgery (NSG), University of Washington, Seattle, Washington

SUMMARY Immunohistochemistry (IHC) is a valuable tool for labeling structures in tissue samples. Quantification of immunolabeled structures using traditional approaches has proved to be difficult. Manual counts of IHC-stained structures are inherently biased, require multiple observers, and generate qualitative data. Stereological methods provide accurate quantification but are complex and labor-intensive when staining must be compared among large numbers of samples. In an effort to quickly, objectively, and reproducibly quantify cutaneous innervation in a large number of counterstained tissue sections, we developed a color subtractive–computer-assisted image analysis (CS–CAIA) system. To develop and test the CS–CAIA method, tissue sections of diabetic (db/db) mouse skin and their wild-type (db/–) littermates were stained by IHC for the neural marker PGP 9.5. The brown-red PGP 9.5 peroxidase stain was colorimetrically isolated through a scripted process of color background removal. The remaining stain was thresholded and binarized for computer determination of nerve profile counts (number of stained regions), area fraction (total area of nerve profiles per unit area of tissue), and area density (total number of nerve profiles per unit area of tissue). Using CS–CAIA, epidermal nerve profile counts, area fraction, and area density were significantly lower in db/db compared to db/– mice.

(*J Histochem Cytochem* 49:1285–1291, 2001)

KEY WORDS

quantification
image analysis
skin
epidermis
nerves
PGP 9.5
immunohistochemistry
diabetic mouse

WHEREAS an antigen can be easily identified using immunohistochemistry (IHC), precise description of differences in staining patterns among sets of tissue samples requires some form of quantification. Quantification of immunohistochemically stained tissue sections has involved four methods: (a) manual counts or ratings by multiple observers of immunolocalized structures by direct microscopic observation generate a semi-quantitation of the structure's frequency, pattern, or intensity (Olerud et al. 1995); (b) stereologic analysis of 2D images by counting intersections between imposed grids and stained structures (Oorschot and Jones 1991; Coggeshall and Lekan 1996) results in a quantitative description of structures in a 3D volume derived from 2D images; (c) a 3D volume can be reconstructed using an optical sectioning method, such

as laser scanning confocal microscopy of thick tissue sections or whole mounts with subsequent tracing and measurement; (Kennedy et al. 1996; Kennedy and Wendelschafer–Crabb 1999); and (d) profile measurements using computer-assisted image analysis (CAIA) facilitate the separation of the tissue elements of interest from background, using differences in size, shape, density, brightness, texture, or color (Hughes and McCulloch 1991; Russ 1995). CAIA allows extraction of 2D feature data such as feature count (number of stained structures), area density (number of features per unit area of interest), area fractions (total area of features per unit area of interest), orientation, shape, and distribution.

Each method has limitations. Manual quantification is labor-intensive and requires multiple observers to adhere to stringent, mutually accepted parameters to maintain inter-observer agreement. Although this method has been successfully used to describe morphological findings such as degree of inflammation (Olerud et al. 1995), it provides only semiquantifiable data.

Correspondence to: Dr. John Olerud, Dept. of Medicine (Dermatology), Box 356524, Seattle, WA 98195-6524.

Received for publication May 4, 2001; accepted June 5, 2001 (1A5540).

Whereas stereology is a well-established and reliable way to derive 3D information or the volume fraction from 2D data sets (West et al. 1991; Gundersen 1992; Saper 1996; Skoglund et al. 1996), it is also prohibitively labor intensive and complex when large volumes of specimens are worked with. When the goal is a comparison of staining among experimental groups, the rigors of stereology may be unnecessary (Coggeshall and Lekan 1996).

Laser scanning confocal microscopy and neuron tracing yield exquisite 3D data but require extensive time and expensive hardware/software, making it difficult to collect data on large numbers of specimens.

Computer-assisted image analysis (CAIA) can be a simple, economical, and effective method of quantification when the goal is to compare staining characteristics among experimental groups. CAIA relies on the ability to cleanly separate or segment a structure of interest from its background using a physical difference, such as color, to facilitate segmentation of red/brown stained nerves in the blue nuclear counterstained tissue sections. Commercially available software and recognized protocols for color segmentation using positive color identification can be used to describe the color of interest and let the computer segment or select the region of the micrograph containing that color. However, our attempts at positive color selection required unique selection parameters for each micrograph and failed to produce accurate segmentation of the epidermal nerves, as determined by visual inspection.

To test our hypothesis that numbers of cutaneous nerves are reduced in the diabetic mouse model compared to their normal wild-type littermates, we pursued a different method, known as color subtractive computer-assisted image analysis (CS-CAIA). CS-CAIA takes the opposite approach, compared to positive color selection, by peeling away non-peroxidase colors through a standardized sequential process of color background removal, leaving the peroxidase-labeled nerves on a white background. By using Photoshop 5.0 (Adobe; San Jose, CA) and the Image Processing Tool Kit 2.5 (Reindeer Games; Asheville, NC) software, we were able to use CS-CAIA to generate fast, consistent morphometric data on various specimens examined by multiple operators.

Materials and Methods

Tissue Preparation and Immunohistochemistry

Equal-sized skin samples were excised from comparable locations on the backs of shaved, genetically diabetic C57BL/Ks J-M^{+/+}Lepr^{db} (db/db) mice and their wild-type (db/−) littermate (Jackson Laboratory; Westgrove, PA) according to a protocol approved by the University of Washington Animal Care Committee. Tissue samples were immediately

fixed in 10% neutral buffered formalin at 4°C for 24 hr, then processed for paraffin sectioning. Six- μ m-thick tissue sections were stained by IHC using an indirect immunoperoxidase method as previously described (Olerud et al. 1998). Briefly, sections were rehydrated and blocked for endogenous peroxidase using 0.3% hydrogen peroxide and nonspecific antibody binding using 2% normal goat serum. The polyclonal primary antibody PGP 9.5 (Accurate; Westbury, NY) was applied at 1:750 dilution for 1 hr. The biotinylated goat anti-rabbit antibody (Vector; Burlingame, CA) was applied at 1:200 dilution for 30 min. Amplification with streptavidin peroxidase (Zymed; San Francisco, CA) was performed according to the manufacturer's instructions. Sections were developed in 0.12% 3',5'-diaminobenzidine in Tris buffer for 20 min and counterstained with Lerner's Hematoxylin (Lerner Laboratory; Pittsburgh, PA).

Imaging

Tissue sections were viewed using brightfield illumination on a Nikon SA Microphot upright light microscope with a $\times 20$ plan-apochromatic objective with a numerical aperture of 0.75. Images were captured through consecutive red, green, and blue separation filters on a Photometrics Sensys monochrome digital camera with a grade 1 KAF 1400 CCD. Image acquisition was controlled through IPLab Spectrum software (Scanalytics; Vienna, VA) running on a Power Mac 9600 MP-200 computer. The separate 1317 \times 1035 pixel 12-bit grayscale images were merged and saved as a 24-bit color TIFF file.

Color Subtractive Computer-Assisted Image Analysis

The Image Processing Tool Kit version 2.5 was loaded into the Photoshop 5.0 plug-ins folder. After restarting the computer, the image processing tools appear under the "Filter" menu within the Photoshop program. Scripting, to create a set of "actions," was performed according to instructions in the Photoshop 5.0 manual. Briefly, with an image file open, the record button in the Photoshop action palette was activated to record command choices that were then saved as a "script." The scripts that are recorded and saved can be loaded into the action palette, where the functions are performed by pressing the "Play" button. The sequence of scripted actions described here relates to the separation and measurement of immunoperoxidase-stained epidermal nerves in a $\times 20$ -imaged field.

Calibration. A stage micrometer was used to determine that the distance across the imaged $\times 20$ field was 369 μ m. Image files were opened in Photoshop 5.0. The image was spatially calibrated using the "calibration filter" (Filter>IP Measure>Calibrate) marking two reference points at the opposing edges of the field and entering the known calculated distance of 369 μ m (Figure 1A).

Epidermal Mask. In a new layer (Layers Palette>Create New Layer) named "Epidermal mask" the user was prompted to use a black pencil to delineate the region of interest, in our case the epidermis. The interior of the outlined epidermis was selected with the magic wand tool (non-alias) and filled with black (Edit>Fill>Black 100%). The exterior of the epidermis was selected and filled with white using the

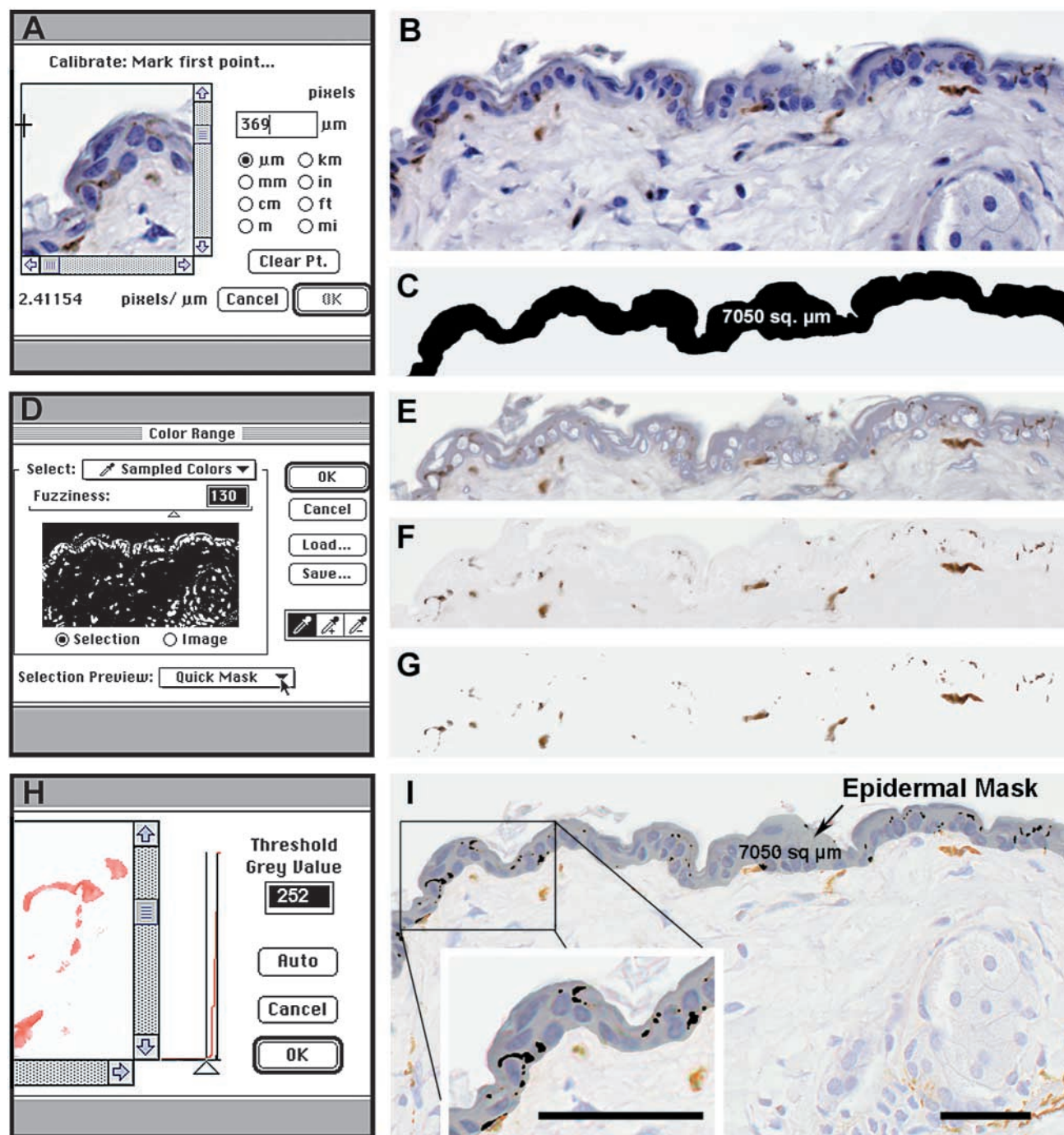


Figure 1 (A,B) The image is calibrated using the "calibration filter." (C) The epidermis is delineated and its area calculated. (D) Using the "color range" command, non-peroxidase colors are sampled, fuzziness set, and the selected areas are filled with white. (E-G) The color subtraction process is repeated until the colors of non-peroxidase-stained structures are replaced by the white homogeneous background. (H,I) The image is thresholded and boolean logic is used to display only the nerves in the epidermis. Bars = 50 μm .

same method. Because features that touch the edge of the field were not measured, the black epidermal mask was delineated from the right and left edges of the field with straight white pencil lines. The area of the epidermis was calculated and recorded using "Feature ID" (Filter>IP Measure>Feature ID>Area) (Figure 1C). This epidermal area

measurement was later used to normalize the number of nerve profiles per epidermal area.

Color Subtraction. This color subtraction sequence removed the non-peroxidase background colors by replacing them with white (Figures 1E-1G). The layer containing the

image of the tissue section was selected, duplicated, and the new layer was named “color subtraction.” Using the color sampler tool (5×5 pixel average), the darkest most opposite hue (blue nuclei) compared to the red/brown peroxidase hue was sampled by clicking the cursor on that color. “Color range” (Select > Color Range) was used after each color sampling to select all pixels in the image that are similar to the sampled color using a sliding scale called “Fuzziness” (Figure 1D). Fuzziness can be thought of as the color range or bandwidth that will be accepted in the segmentation using the color sample as the reference. The color of the selected pixels was replaced with white (Edit>Fill>White>100% Normal). This same color selection and replacement can be achieved using the “Replace Color” tool (Image>Adjust>Replace Color). Color selection and replacement as part of the same tool allows a more interactive visual method. This subtraction process was repeated until all non-peroxidase colors were replaced with white. Setting fuzziness values higher for the first dark blue hematoxylin colors (nuclei), then progressively lower for the intermediate and lighter colors, appeared to be optimal. This progressive specificity prevents the color subtraction from removing the brown/red color of interest. Fuzziness thresholds for the image in Figure 1 were set at a progression of 150, 130, 100, and 50. The subtraction sequence was incorporated into the script, saved, and tested on a representative image set. This test is necessary to ensure the script’s ability to accommodate all the variations of brightness, contrast, and hue that will be encountered in the full set of images for analysis. After the color subtraction sequence was run on an image, the immunoperoxidase-stained nerves stood out against the homogeneous white background.

Thresholding. The “color subtraction” layer was duplicated and the new layer was named “threshold.” With the nerves displayed on a white homogeneous background, simple bi-level thresholding was performed (Filter>IP Measure>Bi-threshold) (Figure 1H). A target value of 252 was set in the threshold window. By clicking “OK” the user converted the image to strictly black or white (binary). Values above the target threshold resulted in white pixels, whereas values that fell on or below the target threshold resulted in groups of black pixels representing the stained nerves. In this study, the pretested threshold target value of 252 faithfully profiled the areas of nerve staining.

Opening Filter and Cutoff Filter. The binary image contained single and small groups of black pixels representing peroxidase label at the fringes of a nerve profile or residual background. Unless this “shot” background was selectively removed, each black pixel or group of pixels was counted as a feature, distorting the overall feature count. To selectively remove the shot background, an “opening filter” or “cutoff filter” was used. The “opening filter” (Filter>IP Morphology>Open) eroded the perimeter of all features by one pixel depth, then dilated the features by one pixel. Single and small groups of pixels disappear when eroded, becoming unavailable for dilation, and were thereby permanently removed. The alternative “cutoff filter” (Filter>IP Measure>Cutoff) removed black pixel groups that were below a designated number. Both methods for removing the “shot” background worked well, and features that remained after

the “opening” or “cutoff” were visually identified as nerves and retained their original areas.

Boolean “And.” Boolean logic was used to identify the segmented structures that existed only within the epidermis. The “epidermal area” layer that was created at the beginning of the script sequence was selected and “set up as second image” (Filter>IP Boolean>Set Up Second Image). This held the epidermal image in memory for subsequent comparison with the image containing the nerve profiles. The “threshold layer” was then selected and a Boolean “And” function (Filter>IP Boolean>And) was performed to display the structures that co-existed in both images, i.e., nerves in the epidermis. This image was saved as a new layer called “epidermal nerves” (Figure 1I).

Feature Data. Feature measurements were done on the binary images in which black pixels were measured and white pixels were not. The layer called “epidermal nerves” was selected and the feature data (Filter>IP Measure>Feature Data) was saved from this image for subsequent analysis. The saved feature data included feature counts, areas, lengths, breadths, orientations, positions, and shapes. Data used for our analysis included only the feature counts and the corresponding feature areas in square micrometers. The feature data file was opened in a database or statistical program for further analysis.

Statistical Analysis. Differences between experimental groups were determined using a one-way analysis of variance (ANOVA). Data were logarithmically transformed to adjust for heteroscedasticity in distribution. Charted data are expressed as means \pm SE.

Results

The average area density (total number of nerve profiles per unit area of epidermis) for the db/– mice was 5529 nerve profiles/mm² compared to the average db/db area density of 2044 nerve profiles/mm² of epidermis. The average area fraction for the (db/–) mice was 1.9% compared to db/db mice at 0.49%.

Area densities derived from littermates (db/–) and diabetic mice (db/db) manually counted by three observers show some expected inter-observer variability (Figure 2A). The results of area density and area fraction measurements derived from the three observers using CS-CAIA on the same set of images shows closer agreement (Figures 2B and 2C). The remaining variability is attributable to the human choice in demarcating the epidermal boundaries. A significant difference in epidermal innervation between db/– and db/db was detected by the manual counts of the three observers ($p=0.02$) (Figure 2A). Significant differences detected by the three observers using CS-CAIA show $p=0.011$ for area density and $p=0.003$ for area fraction (Figures 2B and 2C).

Using CS-CAIA and a larger data set of 20 images each of db/– and db/db mice shows $p < 0.001$ for both area density and area fraction (Figure 3). These

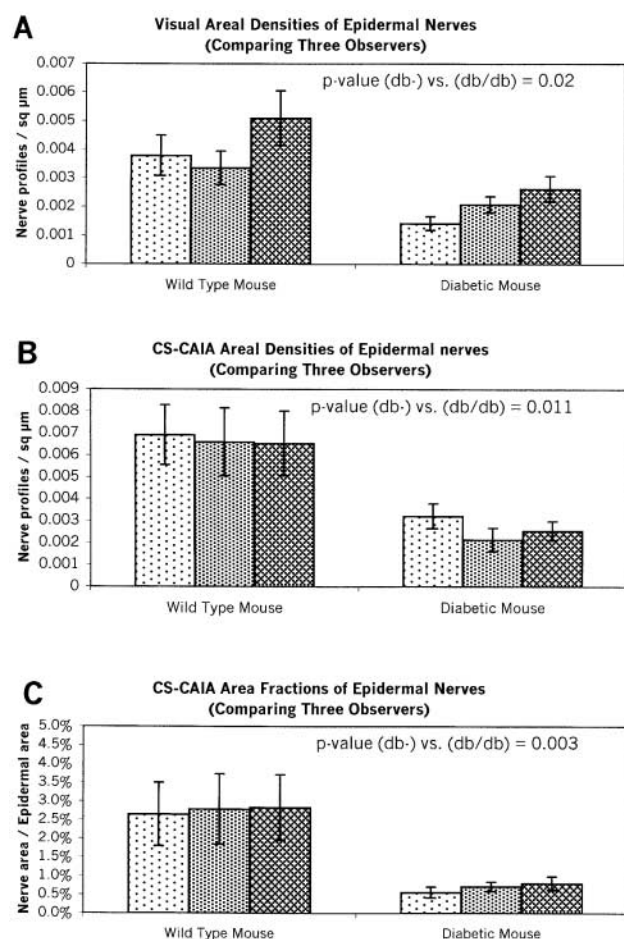


Figure 2 (A) Data comparing three observers' manual counts of epidermal nerves from nine micrographs each of wild-type and diabetic mice. Experimental vs control $p=0.02$. (B) Area densities (epidermal nerve profiles per epidermal area) derived using CS-CAIA are plotted, showing improved inter-observer agreement. Experimental vs control $p=0.011$. (C) Area fractions (area of nerves per epidermal area) of the same data set using CS-CAIA. Experimental vs control $p=0.003$. The remaining variability results from human choice in demarcation of the epidermal boundaries.

data support our hypothesis that diabetic obese mutant mice have fewer epidermal nerves than heterozygous non-diabetic littermates.

Discussion

Kennedy and colleagues (Kennedy et al. 1996; Kennedy and Wendelschafer-Crabb 1999) demonstrated the utility of quantifying epidermal nerves in patients with diabetic neuropathy. The method of quantification for these human studies involved laser scanning confocal microscopy of 50–100 μm -thick tissue sections with subsequent neuron tracing and 3D measurement. This equipment and a time-intensive approach revealed a reduction in total epidermal nerve length (sum of nerve lengths within the epider-

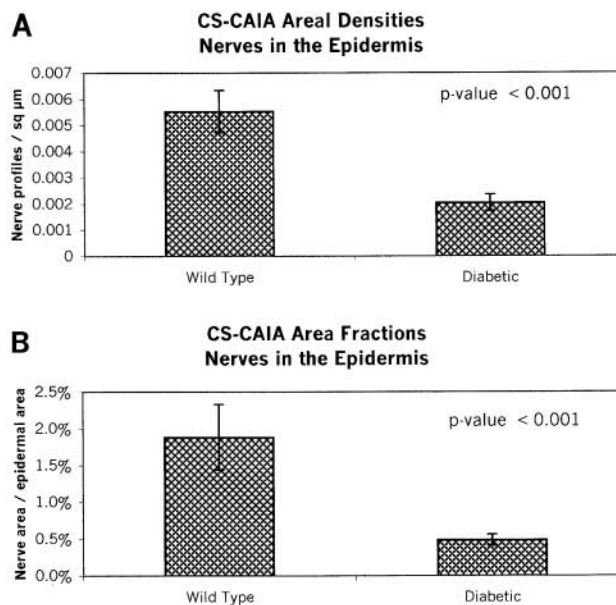


Figure 3 (A) Area density comparison of wild-type (db/-) littermates to the diabetic (db/db) mice shows reduction in number of nerves in the db/db mouse epidermis. Experimental vs control $p<0.001$. (B) Area fraction comparison of wild-type (db/-) littermates to the diabetic (db/db) mice shows reduced epidermal area occupied by nerves in the db/db mouse. Experimental vs control $p<0.001$.

mal volume) and number of nerve origins (nerve trunks crossing the basement membrane) in epidermis from patients with diabetic neuropathy compared to normal epidermis. Our method using 5- μm tissue sections, routine immunoperoxidase staining, standard light microscopy, and easily accessible software also shows the predicted reduction in epidermal nerves in diabetic (db/db) mice compared to non-diabetic littermates. Although our method does not elucidate the morphological characteristics of epidermal nerves in three dimensions, it does, simply and economically, address the differences in the extent of epidermal innervation. Kennedy and colleagues observed no significant difference in ratios of nerve branches per nerve length comparing diabetic and normal human epidermal nerves (Kennedy et al. 1996; Kennedy and Wendelschafer-Crabb 1999). This suggests that nerve profile area density measurements provide a reliable representation of overall epidermal innervation without being skewed by differences in nerve branching frequency or nerve length. CS-CAIA is a simple method of obtaining these measurements.

CD-CAIA has been previously performed in two ways. The first method separates the RGB (red, green, and blue) image into its grayscale components. If the color of interest is clearly delineated in one of the images, simple thresholding can be performed. If the color is a more complex mixture, which is usually the

case, the delineation is enhanced by defining percentages of color mixes or individually thresholding the RGB grayscale components and recombining the images using boolean logic to display only areas that overlap (Bacus et al. 1988; Shapiro et al. 1992; Yamamoto et al. 1992; Kuyatt et al. 1993; Willemse et al. 1993,1994; Fritz et al. 1995; Ruifrok 1997). The second method converts the RGB image into HSI (hue, saturation, and intensity). Using the hue (thought of as wavelength of color) and saturation (amount of color), an approximation of human color perception is made without the added variable of the gray value component (Goto et al. 1992; Defigueiredo et al. 1995; Kohlberger et al. 1996).

With these methods, positive descriptions of color must be broad enough to include all the features of interest and strict enough to exclude background. This scenario creates a color description that is often specific to each image, exhibiting impaired accommodation of variations in color hues among different images. Our attempts at positive color selection resulted in segmented features (nerves) that were not discrete areas of stain but were excessively fragmented. Fragmented features distorted the feature count and area density measurements, as each small group of pixels becomes part of the feature count. Without a sophisticated software program that could learn to accommodate a large set of images, it was prohibitively laborious for a single operator to analyze hundreds of images.

CS-CAIA allows greater latitude in using the software tools to remove unwanted colors. The CS-CAIA script can include color subtraction sequences removing colors that may exist in the image set as a whole and not in a specific image. Therefore, CS-CAIA can be used as a generic script accommodating a larger, more diverse image set. However, CS-CAIA is sensitive to color shifts of the peroxidase stain if the color becomes similar to background hues that are targeted for removal.

As with most computer scripts or macros, human operators must verify the results. Operators must understand the commands being executed by the script and be able to evaluate when the operations or parameters are not appropriate. To test the performance of scripts, three independent investigators quantified nerves in the epidermis in the same set of anonymous image files. Comparisons of the three data sets revealed steps in the process that contributed to variability. Five sources of variability were identified: (a) differences in defining the epidermal boundaries; (b) overly specific color subtraction sequence that required the operator to subsequently remove remaining background colors in some images; (c) arbitrary adjustment of the threshold value. Target values must be tested and are dependent on the tonal contrast transi-

tioning from the background white to the remaining tones or colors representing the structures of interest; (d) opening the image file using different Photoshop color conversions causing the script to exhibit altered color removal; and (e) capturing images with variations in microscope parameters and alignment can cause image artifacts beyond the script's ability to accommodate.

We incorporated several changes to control these variables. (a) Definitions for the morphological boundaries of the epidermis were determined by group consensus. Care was taken to ensure that the outside edge of the pencil line tool delineated the epidermal area rather than the middle or inside edge of the line. If the line tool is several pixels thick, the area of the epidermis can be erroneously increased. (b) Scripts were tested on larger set of images, avoiding the need for subsequent removal of remaining background colors. (c) The threshold level was set to the absolute value of 252, avoiding arbitrary thresholding. (d) Images were opened using the same Photoshop color conversion scheme. (e) Microscope alignment, lamp voltage, filtration, and image capture were tightly controlled.

In conjunction with controlling these variables, certain scripting features were incorporated to avoid the hazard of letting scripts churn out aberrant data. After a script is loaded, the Photoshop action palette displays the list of commands that will be carried out. To the left of each command is a checkmark box that can be clicked on or off, allowing that command to be performed or omitted when the script runs. Quick adjustments can be made to the script to accommodate variable samples. This allows alternate subtraction sequences to be incorporated into the script, enabling quick editing of the color subtractions. Another useful feature of the script is the ability to insert "stops." These "stops" interrupt the script and can display instructions to the operator when operator input is required. Insertion of stops greatly enhances the usability of the script by multiple operators. The final check should always be the visual correlation between the segmented feature profile and the peroxidase-labeled structure in the micrograph. This check can be incorporated into the script by selecting the "threshold layer," "select all," "copy," and "paste" into the micrograph layer. The opacity of the threshold layer can then be set to 50%, allowing the operator to view the segmentation as an overlay. This provides the opportunity to easily distinguish appropriate correlation between the original micrograph and the thresholded profile. After incorporation of the CS-CAIA parameters, the standard deviation existing in data generated by multiple operators remains directly attributable to the remaining variable of defining the boundaries of the epidermis.

We have come to several conclusions. First, CS-CAIA

yields data that can be easily normalized to the region of interest (e.g., epidermal area). Second, CS-CAIA reduces human bias. CS-CAIA enhances segmentation with integration of enhancement tools and analysis tools, thus eliminating the need of working among multiple software programs to achieve desired segmentation and measurement. CS-CAIA is more accommodating to heterogeneity in the color of interest and allows increased latitude in color removal. CS-CAIA decreases training time because the entire process occurs within a single software environment. Variations in nerve counts from image to image indicate the need for high sampling rate. Pooling the feature data from multiple sections, images, and mice will supply the necessary statistical power to facilitate the comparison of experimental vs control groups. Although we have used quantification of nerves for this study, the CS-CAIA method will allow quantification of a variety of stained structures.

Impaired wound repair in patients with diabetes is of major concern and the role of innervation is of key interest. Our murine studies correlate well with our previous observations that humans with diabetes demonstrate reduced numbers of cutaneous nerves. CS-CAIA objectively quantifies structures of interest, such as nerves, and provides a valuable tool to enhance our understanding of the relationship between nerves and the diabetic phenotype.

Acknowledgments

Supported by NSF EEC 9529161, NIH RO1 HD33024-05, NIH CA49259, NIH AR-21557, RO1 GM56483-01, and the Odland Endowed Chair.

Special thanks to Holly Predd and Dr Stephen Sullivan for expert technical assistance and to Marc Antezana for editorial support in this project.

Literature Cited

- Bacus S, Flowers JL, Press MF, Bacus JW, McCarthy KS Jr (1988) The evaluation of estrogen receptor in primary breast carcinoma by computer-assisted image analysis. *Am J Clin Pathol* 90:233-239
- Coggeshall RE, Lekan HA (1996) Methods for determining numbers of cells and synapses: a case for more uniform standards of review. *J Comp Neurol* 364:6-15
- Defigueiredo RJP, Cummings BJ, Mundkur PY, Cotman CW (1995) Color image analysis in neuroanatomical research: application to senile plaque subtype quantification in Alzheimer's disease. *Neurobiol Aging* 16-2:211-223
- Fritz P, Wu X, Tukzek H, Multhaupt H, Schwarzmann P (1995) Quantification in immunohistochemistry. a research method or a diagnostic tool in surgical pathology? *Pathologica* 87:300-309
- Goto M, Nagatomo Y, Hasui K, Yamanaka H, Murashima S, Soto E (1992) Chromaticity analysis of immunostained tumor specimens. *Pathol Res Pract* 188:433-437
- Gundersen HJG (1992) Stereology: the fast lane between neuroanatomy and brain function or still only a tightrope. *Acta Neurol Scand Suppl* 137:8-13
- Hughes FJ, McCulloch CAG (1991) Quantification of chemotactic response of quiescent and proliferating fibroblasts in Boyden chambers by computer assisted image analysis. *J Histochem Cytochem* 39:243-246
- Kennedy WR, Wendelschafer-Crabb G (1999) Utility of the skin biopsy method in studies of diabetic neuropathy. *Clinical neurophysiology: from receptors to perception. EEG (suppl 50):553-559*
- Kennedy WR, Wendelschafer-Crabb G, Johnson T (1996) Quantification of epidermal nerves in diabetic neuropathy. *Neurology* 47:1042-1048
- Kohlberger PD, Obermair A, Sliutz G, Heinzl H, Koelbl H, Breitenacker G, Gitsch G, Kainz C (1996) Quantitative immunohistochemistry of factor VIII-related antigen in breast carcinoma, a comparison of computer-assisted image analysis with established counting methods. *Anat Pathol* 105:705-710
- Kuyatt BL, Reidy CA, Hui KY, Jordan WH (1993) Quantification of smooth muscle proliferation in cultured aorta; a color image analysis method for the Macintosh. *Anal Quant Cytol Histol* 15:83-87
- Olerud JE, Chiu DS, Usui ML, Gibran NS, Ansel JC (1998) Protein gene product 9.5 is expressed by fibroblasts in human cutaneous wounds. *J Invest Dermatol* 4:565-572
- Olerud JE, Odland GF, Burgess EM, Wyss R, Fisher LD, Matsen FA III (1995) A model for the study of wounds in normal elderly adults and patients with peripheral vascular disease of diabetes melitus. *J Surg Res* 59:349-360
- Oorschot DE, Jones DG (1991) Neuronal survival and neurite growth in cultured cerebral explants: assessment of the effect of cytosine arabinoside using improved stereology. *Brain Res* 546:146-150
- Ruifrok AC (1997) Quantification of immunohistochemical staining by color translation and automated thresholding. *Anal Quant Cytol Histol* 19:107-113
- Russ JC (1995) *The Image Processing Handbook*. 2nd ed. Boca Raton, FL, CRC Press
- Saper CB (1996) Any way you cut it: a new journal policy for the use of unbiased counting methods. *J Comp Neurol* 364:5
- Shapiro E, Hartanto V, Lepor H (1992) Quantifying the smooth muscle content of the prostate using double-immunoenzymatic staining and color assisted image analysis. *J Urol* 147:1167-1170
- Skoglund TS, Pascher R, Berthold CH (1996) Aspects of the quantitative analysis of neurons in the cerebral cortex. *J Neurosci Methods* 70:201-210
- West MJ, Slomianka L, Gundersen HJG (1991) Unbiased stereological estimation of the total number of neurons in the subdivisions of the rat hippocampus using the optical fractionator. *Anat Rec* 231:482-497
- Willemsse F, Nap M, Eggink HF (1993) Image analysis in immunohistochemistry. *Anal Quant Cytol Histol* 15:136-143
- Willemsse F, Nap M, Henzen-Logmans SC, Eggink HF (1994) Quantification of area percentage of immunohistochemical staining by true color image analysis with application of fixed thresholds. *Anal Quant Cytol Histol* 16:357-364
- Yamamoto K, Makino Y, Yoshioka T, Kobashi H, Tomita M, Tsuji T (1992) Quantitative analysis of activated Kupffer cells in viral hepatitis: application of computer image analysis for lectin histochemistry. *Liver* 12:199-204